Journal of the Korean Ceramic Society
Vol. 31, No. 1, PP. 104~114, 1994.

Fabrication of Y_2O_3-ZrO_2 and CaO-ZrO_2 Fibers by Sol-Gel Process and Their Phase Characterization by Raman Microprobe

Chin Myung Whang, Hee Tai Eun and Hyeok Kee Kwon
Dept. of Ceramic Engineering, Inha University
(Received September 22, 1993)

졸-겔법에 의한 Y_2O_3-ZrO_2계와 CaO-ZrO_2계 섬유의 제조 및 Raman Microprobe에 의한 상분석

황진명 · 은희태 · 권혁기
인하대학교 무기재료공학과
(1993년 9월 22일 접수)

ABSTRACT

ZrO_2 fibers were fabricated by means of the Sol-Gel process using $Zr(O\text{-}nC_3H_7)_4$-H_2O-C_2H_5OH-HNO_3 solution as a starting material. The optimum experimental parameters such as molar ratio of starting materials, concentration, temperature. viscosity, the amounts of stabilizer and the pH of solution were determined. The experimentally determined optimum variables which produce good ZrO_2 fibers were used to manufacture the Y_2O_3- and CaO-ZrO_2 fibers. The amounts of Y_2O_3 and CaO were varied within the range from 1.5~5 mol% and 3~15 mol% respectively. The phase transformation and microstructural evolution of the fabricated ZrO_2 gel fibers were investigated after heat treatments up to 1200℃ by X-ray diffraction, Raman microprobe spectroscopy, SEM, and specific surface area and pore volume measurements. From the analysis of X-ray diffraction and Raman spectra, the phase of heat treated Y_2O_3- and CaO partially stabilized ZrO_2 gel fibers(Y_2O_3:2.5~3 mol%, CaO:6~9 mol%) were identified as a tetragonal phase up to 1000℃. The maximum tensile strength of $2.5Y_2O_3$-$97.5ZrO_2$ and 6CaO-$94ZrO_2$ (in mol%) fibers heat treated at 1000℃ for 1 hr was found to be 1.3~2 GPa with diameters of 10~20 μm.

요 약

본 연구에서는 $Zr(O\text{-}nC_3H_7)_4$-H_2O-C_2H_5OH-HNO_3 용액을 출발물질로하여 지르코니아 섬유를 제조하였고 섬유 제조에 요구되는 제 실험변수-출발물질의 몰비, 농축온도. 점도, 안정화제의 양, pH-를 결정하였다. 가장 좋은 조건에서 섬유를 얻었을 때의 실험변수를 고정시켜 안정화제로 Y_2O_3, CaO를 지르코니아에 고용시킨 지르코니아 섬유를 제조하였다. 사용된 Y_2O_3와 CaO의 양은 각각 1.5~5 mol%와 3~15 mol%였다. 제조된 지르코니아 겔 섬유를 1200℃ 까지 열처리하면서 온도 변화에 따른 특성을 XRD, Raman microprobe 분광분석, SEM, 비표면적, 세공용적, 미세구조 분석을 통하여 조사하였다. 2.5~3 mol% Y_2O_3와 6~9 mol% CaO가 안정화제로 첨가된 지르코니아 겔 섬유는 1000℃ 까지 정방정상만이 존재하는 것이 XRD와 Raman microprobe 분석결과 밝혀졌다. 1000℃, 1시간 동안 열처리한 2.5 mol% Y_2O_3 및 6 mol% CaO가 첨가된 지르코니아 섬유의 강도는 10~20 μm의 직경에서 각각 1.3~2.0 GPa로 높은 강도를 나타내었다

1. Introduction

Zirconia has excellent properties such as high refractoriness, high mechanical toughness, corrosion resistance, and high wear resistance useful for advanced materials. Considerable attention has been given to fabricate ZrO_2 fibers which are thought to be one of the potential candidates for reinforcement of ceramic and metal bodies, through Sol-Gel process[1-9].

In the present study, we investigated the experime-

ntal variables such as the molar ratio of starting materials, viscosity, reaction temperature, the amounts of stabilizer and the pH of solution for making fiberizable zirconia solutions.

The gel fibers were drawn by immersing a glass rod into the viscous sol prepared under the predetermined optimum experimental conditions for fiber drawing and pulling it up by hand. The optimum amounts of Y_2O_3 and CaO used as stabilizing agents to obtain good mechanical property of the ZrO_2 fiber were determined. The drawn gel fibers were heat treated up to 1200℃ for 1 hr

We measured the specific surface area, pore volume, and tensile strength of the Y_2O_3- and CaO-partially stabilized gel fiber. The studies on phase transformation and microstructural evolution of the gel fibers which depend markedly on the amounts and type of dopant, the heat treatment involved and the cooling process were carried out by means of X-ray diffraction, Raman microprobe spectroscopy, and SEM. The Raman spectra of single crystal and polycrystalline of pure ZrO_2 and Y_2O_3-ZrO_2 systems have been reported[10-11]. So far, no study on the phase transformation of zirconia fibers using Raman microprobe spectroscopy suitable for nonfracture analysis of inorganic fibers has been reported.

In the present work, we report the Raman spectra of pure ZrO_2, $3Y_2O_3$-$97ZrO_2$ and 9CaO-$91ZrO_2$ gel fibers heat treated at various temperatures obtained from Raman microprobe spectrophotometer.

2. Experimental

2.1. Preparation of gel fibers

The zirconia sol solutions and the compositions of which are given in Table 1 are prepared according to the flow diagram shown in Fig. 1.

The molar ratios of H_2O/alkoxide and C_2H_5OH/alkoxide range from 1.0 to 5.0 and from 26 to 49, respectively. $Zr(O\text{-}nC_3H_7)_4$ and absolute ethanol were mixed and stirred in a flask at room temperature for 1hr under refluxing. The other mixed solution of H_2O-C_2H_5 OH-HNO_3 was added dropwise to the $Zr(O\text{-}nC_3H_7)_4$-C_2

Table 1. Compositions and Properties of Solutions for ZrO_2

Solution	Compositions (Molar ratio)				Initial pH (25℃)	Concentration time(h.) at 80℃	Spinnability*	Fiber length (cm)
	$Zr(n\text{-}PrO)_4$	H_2O	EtOH	HNO_3				
1	1	1.0	26.4	0.34	3.9	1.2	P	—
2	1	1.0	26.4	1.0	1.5	4.0	G	—
3	1	1.5	26.4	1.3	0.9	4.5	G	—
4	1	1.6	26.4	0.4	3.3	2.7	G	—
5	1	2.0	26.4	0.4	3.0	1.1	G	—
6	1	2.0	26.4	1.3	0.8	4.5	S	10
7	1	2.2	48.7	0.38	2.8	1.3	P	—
8	1	2.5	48.7	0.38	2.9	1.3	P	—
9	1	2.5	26.4	1.3	0.7	4.7	S	20
10	1	2.6	26.4	1.0	1.1	6.1	G	—
11	1	3.0	26.4	1.0	1.0	6.0	G	—
12	1	3.0	26.4	1.3	0.7	5.0	S	90
13	1	3.3	26.4	1.5	0.3	5.2	S	70
14	1	3.9	26.4	1.5	0.5	5.0	S	30
15	1	4.0	26.4	1.4	0.4	6.5	S	40
16	1	4.0	34.7	1.5	0.6	6.0	S	10
17	1	4.5	26.4	1.5	0.4	5.8	S	40
18	1	5.0	48.7	1.5	0.7	4.1	S	50

*S=Spinnable, G=Gelation and no drawing, P=Precipitation

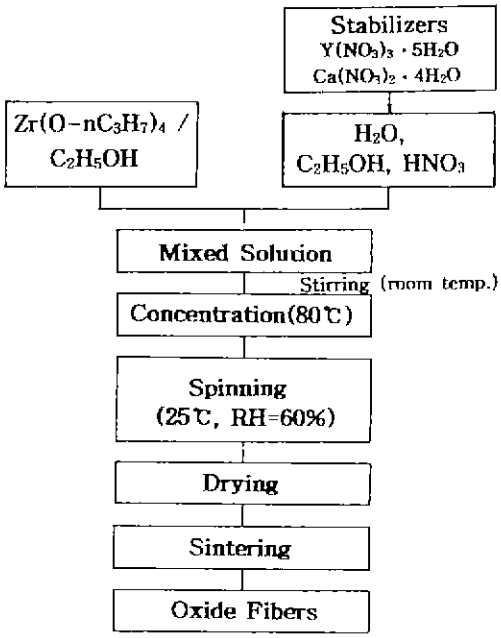

Fig. 1. Flow chart for preparing ZrO_2, Y_2O_3-ZrO_2, and CaO-ZrO_2 fibers through Sol-Gel process.

H_5OH solution using a syringe.

The prepared sol solutions were divided into PE tubes, their pH measured and then concentrated at 80℃ for 4~7 hrs using a waterbath and kept open in ambient air until they became viscous and sticky.

The zirconia gel fibers were drawn from the resultant yellowish viscous sol by immersing a glass rod of about 6mm in diameter and pulling it up by hand. Fibers could be drawn when the viscosity reached above 10 poise as a result of progress of hydrolysis-polycondensation reaction. All processes were carried out in the laboratory under 60% humidity at room temperature. Since fiber drawing is possible only for the alkoxide solutions containing linear polymeric structure, we investigated the optimum conditions of fiber drawing by measuring the viscosities of solution as a function of aging time using LVTDV-II model viscometer.

For the Y_2O_3-ZrO_2 and CaO-ZrO_2 system, yttrium nitrate pentahydrate and calcium nitrate tetrahydrate were used as sources of Y_2O_3 and CaO within the range from 1.5~5 mol% and 3~15 mol%, respectively.

The drawn gel fibers dried in the laboratory for one day at room temperature (below 60% humidity) were heated in air at a heating rate of 1℃/min in the range from 200℃ to 1200℃ and held at various desired temperature for an hour. The heat treated pure zirconia fibers and zirconia fibers containing stabilizing agents were subjected to X-ray diffraction, Micro-Raman, specific surface area, pore volume, tensile strength, and SEM measurements.

2.2. X-ray diffraction measurement

The drawn gel fibers were heated at temperatures ranging from 200℃ to 1200℃ for 1hr and the crystalline phases precipitated in heat treated fibers were identified by means of PW 1710 X-ray diffractometer (Philips Co.). The Ni-filtered CuKα radiation was used as the X-ray source and the measurement conditions were as follows; 20 kV, 25 mA, 20°~80° (2θ).

In the case of coexistence of monoclinic ZrO_2 (m-ZrO_2) and tetragonal ZrO_2 (t-ZrO_2) in fibers, the fraction of t-ZrO_2 was estimated according to the following equation[15].

$$T(\%) = \frac{I_{T(111)}}{I_{M(111)} + I_{M(11\bar{1})} + I_{T(111)}} \quad (1)$$

where I_T and I_M denote the diffraction intensities of t-ZrO_2 and m-ZrO_2 and a set of numbers in the parenthesis are the Miller indices of the diffraction line.

2.3. Raman microprobe spectroscopy

The principal reason for using Raman spectroscopy in this investigation is that the monoclinic and tetragonal polymorphs of zirconia are reported[10-14] to have distinct and characteristic Raman spectra. Also, nondestructive technique by Raman microprobe can be used to characterize the phase and transition temperature in these prepared fibers.

The zirconia fibers were fixed on a cover glass with epoxy and subjected to Raman microprobe analysis using Ramalog-101 spectrophotometer. The spectra of the fibers were recorded for the following conditions; probe diameter ≈2 μm, resolution 1 cm^{-1}, slit width 80 μm. As an exciting line, the 514.5 nm line of an argon laser was used for these experiments and the incident laser power was 100 mW.

The schematic diagram of micro-Raman spectrophotometer is shown in Fig. 2.

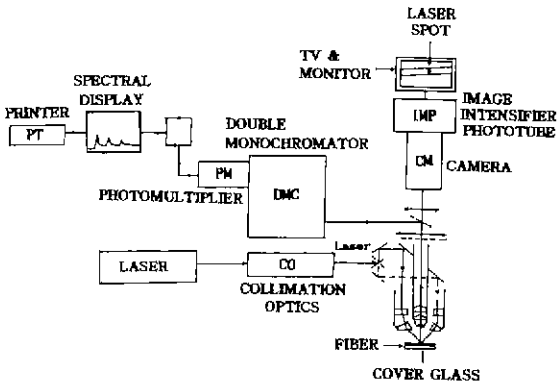

Fig. 2. Layout of the Raman microprobe spectrophotometer.

2.4. Tensile strength measurement

The tensile strength of fibers was measured using an apparatus made in this laboratory to determine the mechanical properties of the fiber. The description of this apparatus was reported in detail elsewhere[17].

A single fiber was set to a rectangular paper (50 mm×10 mm) with epoxy across a diameter of 6mm hole bored at the center. After setting to machine, the paper was cut off at both sides of the hole.

The tensile stress was applied by pulling up the fiber together with an attached weight put on the electric balance. The load velocity was 0.8 g/sec. When the fiber fractured, fracture-load was read from the balance and cross-sectional area was measured under an optical microscope.

3. Results and Discussion

3.1. Spinnability of the sol solution

The properties of the solutions for pure ZrO_2, CaO- and Y_2O_3-ZrO_2 system are listed in Tables 1-3.

The term "P" and "G" in the "spinnability" column indicates that the precipitation(P) and gellation(G) occurred in the solution during the course of reaction.

Recently, Kamiya *et al.*[7] reported spinnability of the sol was accomplished by limiting the amount of water added to the sol to a $H_2O/Zr(O\text{-}nC_3H_7)_4$ molar ratio of 0.7~1.5. In our study, however, we observed the spinnability in the solutions only at $H_2O/Zr(O\text{-}nC_3H_7)_4$ and $HNO_3/Zr(O\text{-}nC_3H_7)_4$ molar ratios of 2~5 and 1.3~1.5, respectively. When the molar ratio of $H_2O/Zr(O\text{-}nC_3H_7)_4$ reached 5, a color change of gel fiber from transparent to opaque was observed during fiber drawing under the 60% relative humidity.

It seems to us that the uptake of the moisture from the ambient atmosphere resulting in the more amount of water consumed than initially added might have contributed to a color change of fiber during the fiber drawing. When we repeated the same experiment under controlled relative humidity of 40%, transparent gel fiber having relatively short length of 5 cm was obtained. Therefore, in our present study, optimum molar ratios of $H_2O/Zr(O\text{-}nC_3H_7)_4$ at ambient temperature with 60% relative humidity is determined to be 3~4 which is a rather large value of water content compared to the one reported by Kamiya[7].

Since the gel fiber could be drawn only from the sol whose initial pH was about 0.8 ($HNO_3/Zr(O\text{-}nC_3H_7)_4$ molar ratio=1.3~1.5), we believe that structure of sols prepared at pH values below 1 is close to linear polymeric structure.

Linear polymer structures proposed by Sakurai[9] (I) and Bradley (II)[18] are as follows.

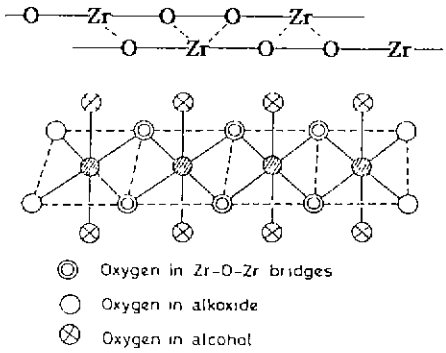

(I) (II)

At this point, there is no consensus as to which of these two structure is correct. More structural study is required to determine the linear polymer structure of zirconia fiber confidently.

Fig. 3 shows the variation of viscosity of $Zr(O\text{-}nC_3H_7)_4$ solutions (molar ratio of water to $Zr(O\text{-}nC_3H_7)_4$=3) as a function of aging time for different reaction temperature.

When hydrolysis-concentration was conducted at 40 ℃, viscosity of the solution increases very slowly during the first 20 hours of aging time. After 20 hours,

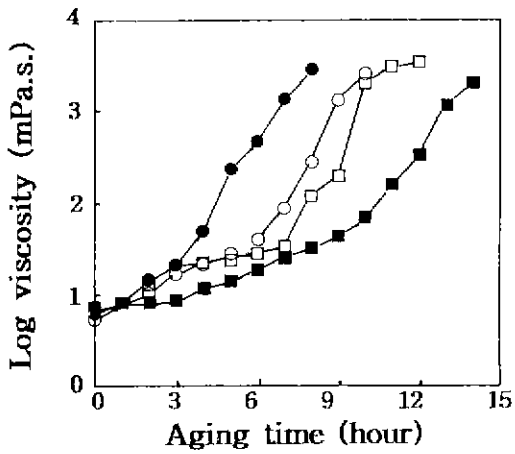

Fig. 3. Variation of viscosity of $Zr(n\text{-}OC_3H_7)_4$ solutions with the molar ratio of $H_2O/Zr(n\text{-}OC_3H_7)_4=2$, 3, 4, 5 at 80℃ as a function of time (●—●: 5, ○—○: 4, □—□: 3, ■—■: 2).

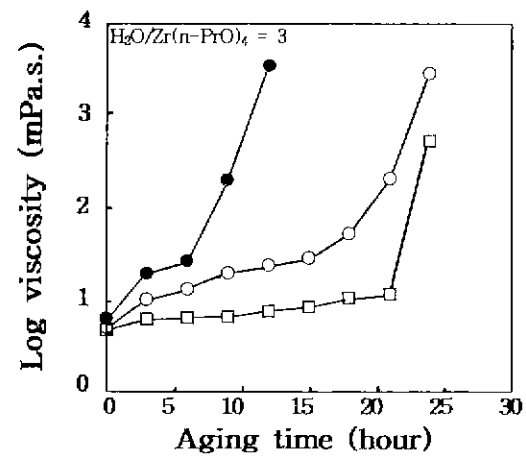

Fig. 4. Variation of the viscosity of $Zr(n\text{-}OC_3H_7)_4$ solutions with the molar ratio of $H_2O/Zr(n\text{-}OC_3H_7)_4=3$ at 40℃, 60℃, and 80℃ as a function of time (●—●: 80℃, ○—○: 60℃, □—□: 40℃).

however, viscosity increased dramatically, so a gel fiber can't be drawn because of gellation.

The time required for a solution to reach the drawable state is 15 hours at 60℃ and 5 hours at 80℃. It was thought that 5 hours is resonable time period for practical application of procedure. Therefore, we determined 80℃ as a optimum reaction temperature.

Fig. 4 illustrates the change in viscosity of $Zr(O\text{-}nC_3H_7)_4$ solutions with the molar ratios of $H_2O/Zr(O\text{-}nC_3H_7)_4=2$, 3, 4, 5 versus aging time for the case in which the reaction temperature was kept constant at 80℃.

Rapid increase in viscosity was observed with the molar ratio of H_2O to $Zr(O\text{-}nC_3H_7)_4=5$, while increase rate was rather slow with the molar ratio of 2. Therefore, the optimum amount of water added to $Zr(O\text{-}nC_3H_7)_4$ was determined to be 3~4. The fiber drawing technique used in this study gave the best results when the viscosity values are between 10~70 poise producing gel fibers of 15~50 μm diameter.

Experimental parameters determined on the basis of results for pure ZrO_2 fibers were used to produce CaO- and Y_2O_3-ZrO_2 fibers in many compositions as shown in Table 2 and Table 3.

$Ca(NO_3)_2\cdot 4H_2O$ and $Y(NO_3)_3\cdot 5H_2O$ were used as sources of CaO and Y_2O_3. The analysis of IR spectra of CaO-ZrO_2 gel fiber is in complete agreement with the previous work reported by Kamiya[7]. IR spectrum of the CaO-ZrO_2 gel fiber suggests that majority of NO_3^- groups are present in ionic state in the gel and

Table 2. Compositions and Properties of Solution for the Y_2O_3-ZrO_2 System

Solutions	Y_2O_3 (mol%)	ZrO_2 (mol%)	Concentration Time (hr.)	Fiber Length (cm)
1.5 YZ	1.5	98.5	4.50	50
2.0 YZ	2.0	98.0	5.00	50
2.5 YZ	2.5	97.5	5.30	40
3.0 YZ	3.0	97.0	5.30	50
4.0 YZ	4.0	96.0	6.00	30
5.0 YZ	5.0	95.0	6.30	30

*Note: Y_2O_3 is added to the No. 12 solution in Table 1.

Table 3. Compositions and Properties of Solution for the CaO-ZrO_2 System

Solutions	Y_2O_3 (mol%)	ZrO_2 (mol%)	Concentration Time (hr.)	Fiber Length (cm)
3 CZ	3.0	97.0	2.30	50
6 CZ	6.0	94.0	3.30	40
9 CZ	9.0	91.0	3.50	40
11 CZ	11.0	89.0	3.50	20
13 CZ	13.0	87.0	6.00	10
15 CZ	15.0	85.0	5.30	5

*Note: CaO is added to the No. 12 solution in Table 1.

only a part of them are attached to Zr covalently in the forms such as monodentate, bidentate and bridging. The covalently bonded structures of NO_3^- group are as follows;

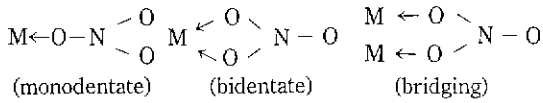

(monodentate) (bidentate) (bridging)

3.2. Crystallization behavior of gel fibers

X-ray diffraction patterns of pure ZrO_2, $3Y_2O_3$-$97ZrO_2$ and $9CaO$-$91ZrO_2$ gel fibers sintered up to 1200℃ for 1hr at intervals of 200℃ are shown in Fig. 5.

The as-drawn gel fibers were X-ray amorphous in all cases. Crystallization behavior of all the gel fibers exhibited first metastable tetragonal phase at temperatures between 200℃ and 400℃. Garvie[16] considered the existance of metastable tetragonal zirconia at room temperature to be related to the structural similarities between the amorphous and the tetragonal phase. So, the tetragonal phase crystallizes easily with low energy. In the case of pure ZrO_2, a small portion of monoclinic phase was found at this stage. The peak intensities of m-ZrO_2 increase as the temperature increases and eventually only monoclinic phase was observed at above 1000℃.

On the other hand, the crystallization behavior of the $3Y_2O_3$-$97ZrO_2$ and $9CaO$-$91ZrO_2$ gel fibers was significantly different from that of the pure ZrO_2 fibers.

In both cases, only tetragonal phase exists up to 1000℃ due to the effect of stabilizers and the slight precipitation of m-ZrO_2 was first observed at 1200℃. The crystallite size effect[16] might be responsible for the appearance of monoclinic phase at this temperature.

Fig. 6 and 7 represent the fraction of tetragonal phase calculated from equation (1) in Y_2O_3-ZrO_2 and CaO-ZrO_2 fibers for different compositions as a function of heating temperature.

It can be seen that the addition of stabilizers inhibits the transformation from tetragonal to monoclinic zirconia. It is clear from the figure that 3 mol% Y_2O_3 and 9 mol% CaO maintain the high fraction of tetragonal phase at high temperature.

Fig. 8 illustrates the Raman spectra observed for sintered fibers of pure ZrO_2, $3Y_2O_3$-$97ZrO_2$ and $9CaO$-$91ZrO_2$ at different heating temperature.

The symmetries of the Raman bands corresponding to the various phases have been previously reported[10-14]. For the tetragonal zirconia (space group D_{4h}^{15}) with two molecules per primitive unit cell, six allowed Raman active modes ($A_{1g}+2B_{1g}+3E_{1g}$) are predicted by factor group analysis. The monoclinic structure (space group C_{2h}^5) has four molecules per unit cell and 18 modes ($9A_{1g}+9B_{1g}$) are expected to be Raman active. On the other hand, the cubic phase has fluorite struc-

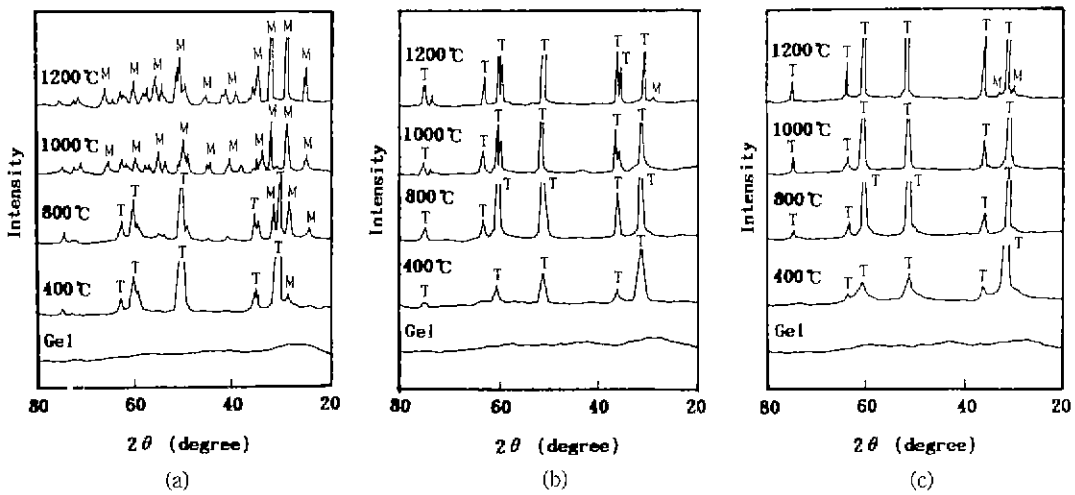

Fig. 5. Variation of X-ray diffraction patterns with different heating temperature for (a) Pure ZrO_2, (b) $3Y_2O_3$-$97ZrO_2$, and (c) $9CaO$-$91ZrO_2$.

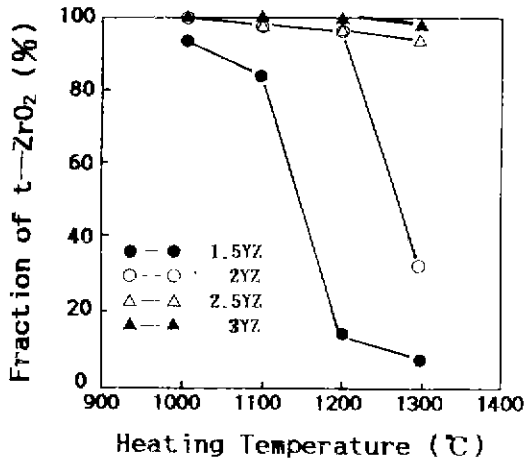

Fig. 6. Change of fraction of tetragonal ZrO_2 phase in Y_2O_3-ZrO_2 fibers for different compositions as a function of heating temperatures.

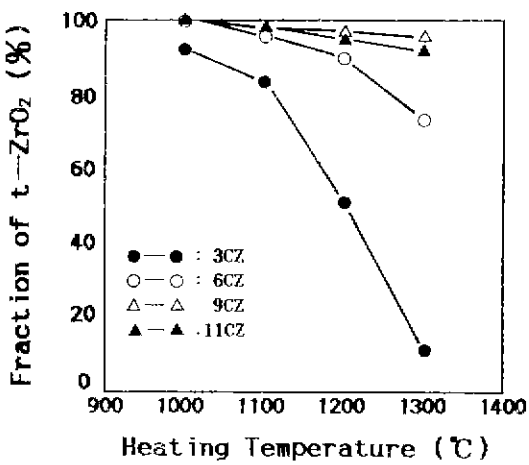

Fig. 7. Change of fraction of tetragonal ZrO_2 phase in CaO-ZrO_2 fibers for different compositions as a function of heating temperatures.

ture (space group O_h^5 : Z=4) and only 1 mode is predicted to be Raman active (F_{2g}).

The peak frequencies of Raman bands for three different fibers are listed in Table 4. The Raman bands observed above 1000 cm^{-1} are identified as the organic and nitrate peaks which disappear completely at above 800℃. Raman peaks originating from monoclinic and tetragonal phase located in the vicinity of one another or overlapped in many lines, especially in excess of 300 cm^{-1}. However, over the range of 100~300 cm^{-1}, the peaks due to two different phases are relatively well separated

The doublet at 181 cm^{-1} and 192 cm^{-1} is the most characteristic of the monoclinic phase and the two strong peaks at 146 cm^{-1} and 264 cm^{-1} are peculiar to the tetragonal phase. These characteristic lines are de-

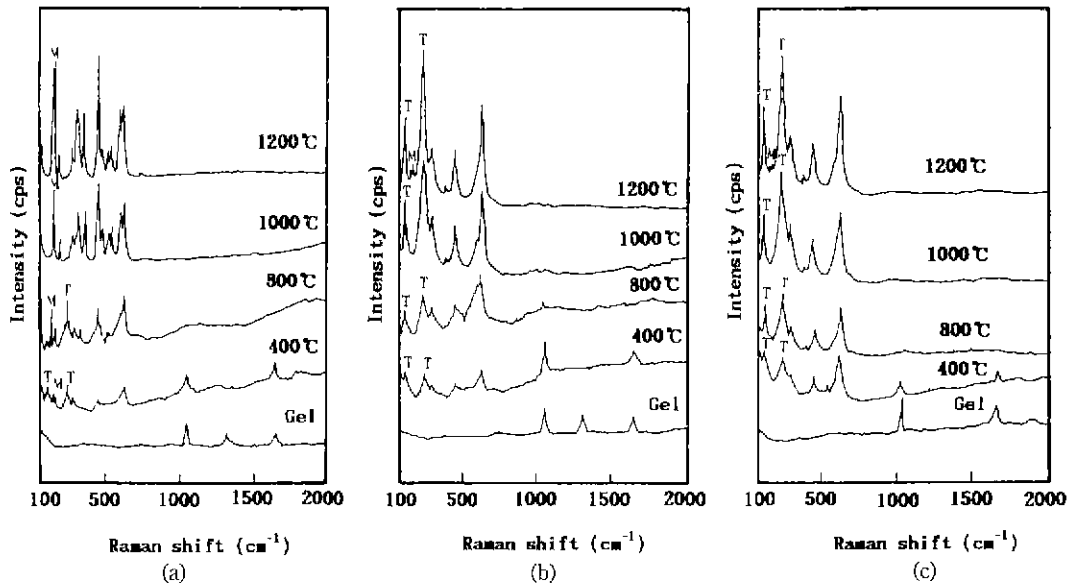

Fig. 8. Raman spectra taken as a function of heating temperatures for (a) Pure ZrO_2, (b) $3Y_2O_3$-$97ZrO_2$, and (c) 9CaO-$91ZrO_2$.

Table 4. Wavenumbers of Raman bands measured for Pure ZrO_2, $3Y_2O_3$-$97ZrO_2$ and 9CaO-91ZrO_2 Fibers Heat Treated at Various Temperatures (cm^{-1})

Temp.(℃) / Fibers	400	600	800	1000	1200
Pure ZrO_2	148 w	148 w	148 br		
	180 br	180 w	180 m	180 s	180 s
	191 br	191 w	191 m	191 s	191 s
			220 w	221 w	220 w
	260 w	261 m	261 m		
				303 sh	303 sh
	319 br		337 br		
				337 sh	337 m
				347 m	347 m
			385 br	385 m	385 m
	473 br	472 w	472 m	476 s	476 s
			503 sh	503 sh	504 sh
			535 sh	535 w	535 w
				560 w	560 w
				618 m	618 s
				637 s	637 s
	645 w	642 m	642 m		
$3Y_2O_3$-$97ZrO_2$	148 br	148 m	148 m	148 s	148 s
					180 br
					191 br
	262 w	261 w	261 m	262 s	260 s
	314 sh	314 sh	315 w	315 w	315 w
				405 br	405 br
	473 br	472 w	473 m	473 m	473 m
			613 w	612 sh	612 sh
	645 w	642 m	645 s	645 s	645 s
9CaO-91ZrO_2	149 br	149 w	149 m	149 m	149 s
					180 br
					191 br
	263 w	263 m	261 s	262 s	262 s
	313 sh	313 sh	313 sh	314 sh	314 sh
				403 br	403 br
	473 br	473 w	473 m	473 m	473 m
			611 sh	611 sh	612 sh
	648 w	648 m	648 s	648 s	648 s

Note: Peak intensity (w: weak, m: medium, s: strong, br: broad, sh: shoulder)

noted as M(monoclinic) and T(tetragonal) in the spectrum, respectively.

The Raman spectrum of pure ZrO_2 fiber at 400℃ indicated tetragonal ZrO_2 with only traces of monoclinic ZrO_2 in accordance with the XRD results.

Since the crystalline state of tetragonal phase is not well developed at this temperature, Raman peaks are relatively ill-defined and broad. As the temperature is raised, the intensity of the characteristic monoclinic doublet increases at the expense of intensity of tetragonal phase.

At 1200℃, the spectrum contains no lines characteristic of the tetragonal phase. It can be attributed completely to the monoclinic phase. Also, the very sharp and strong intensity of monoclinic peaks reflect the degree of crystallinity in this phase.

The monoclinic spectra were distinguished an increase in number of peaks which is predicted to be 18 Raman active modes by group theory. Because of fluorescence, we were not able to observe the band below 100 cm^{-1}, and only 13 Raman active modes are observed.

In the case of Y_2O_3- and CaO-ZrO_2 fibers, analysis of Raman spectra is consistent with XRD analysis, i.e., only tetragonal phase exists up to 1000℃ and a slight precipitation of monoclinic phase occurs at 1200℃. All of 6 Raman active bands appear in the tetragonal phase as anticipated theoretically. A sharpening and increase in the tetragonal intensities takes place as the temperature is raised.

3.3. The properties and microstructures of fibers

Fig. 9 represents the variation of the specific surface area and pore volume of fibers when the amounts of Y_2O_3 and CaO are varied and sintered at 1000℃ for 1 hr.

In the case of 2.5~3 mol% Y_2O_3 and 6~9 mol% CaO, the fibers have the smaller specific surface area and pore volume. But in the case of 4~5 mol% Y_2O_3 and 11 mol% CaO, as more nitrate were added, the values of specific surface area and pore volume increased because of the increase of micropores created from the decomposition of nitrate.

We measured the tensile strength of ZrO_2 fibers containing 2.5 mol% Y_2O_3 and 6 mol% CaO sintered at

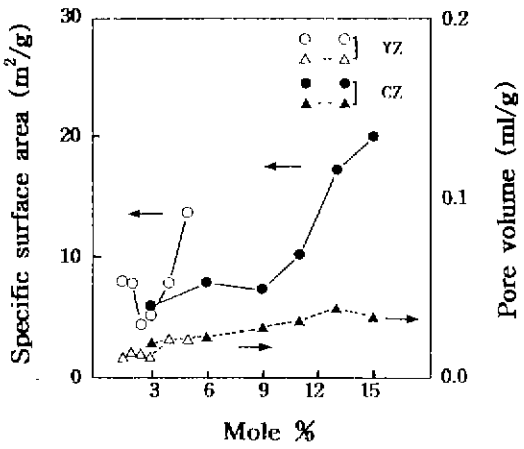

Fig. 9. Specific surface area and pore volume of Y_2O_3-ZrO_2 (mol%) and CaO-ZrO_2 (mol%) fibers plotted as a function of composition sintered at 1000℃ for 1 hr (Open and closed marks stand for Y_2O_3-ZrO_2 and CaO-ZrO_2 fibers, respectively).

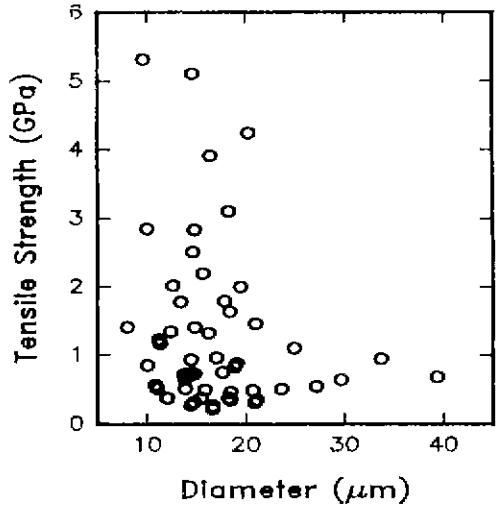

Fig. 10. Tensile strength of 2.5Y_2O_3-97.5ZrO_2 (mol%) fibers sintered at 1000℃ for 1 hr as a function of fiber diameter.

1000℃ for 1hr(Fig. 10 and Fig. 11).

Since hand-drawn fibers by the sol-gel method do not have a constant diameter, strength data are scattered as can be seen in Fig. 10 and Fig. 11. Also, it can be seen that tensile strength of fibers depends on fiber diameter. The larger the fiber diameter is, the smaller the tensile strength of fibers becomes.

The tensile strength of fibers containing 2.5 mol% Y_2O_3 and 6 mol% CaO sintered at 1000℃ for 1hr is about 1.3 GPa and 2.0 GPa at diameter of 10~20 μm, respectively.

Fig. 12 and 13 show SEM photographs of the surfaces of the 2.5Y_2O_3-97.5ZrO_2 and 6CaO-94ZrO_2 fiber sintered at 1000℃ and 1200℃ for 1 hr.

Both fibers sintered at 1000℃ for 1hr retain very smooth surface and fine grained microstructure. However, average grain size of Y_2O_3- and CaO- doped zirconia fiber sintered at 1200℃ for 1hr increased to approximately 0.2 and 0.3 μm, respectively.

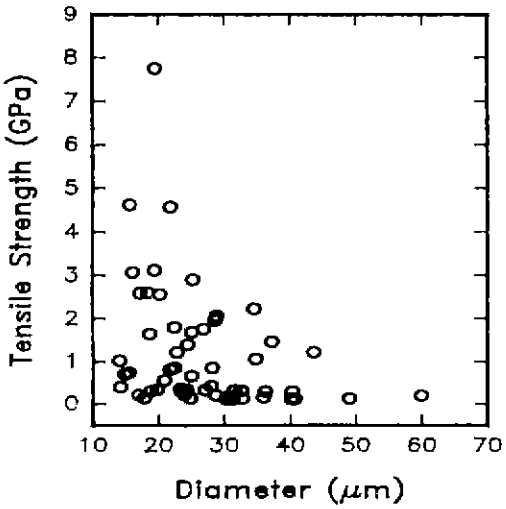

Fig. 11. Tensile strength of 6CaO-94ZrO_2 (mol%) fibers sintered at 1000℃ for 1 hr as a function of fiber diameter.

4. Conclusions

1) The $Zr(O\text{-}nC_3H_7)_4$-H_2O-C_2H_5OH-HNO_3 solutions were prepared and condensed at 80℃. Gel fibers for the $Zr(O\text{-}nC_3H_7)_4$ solutions with the $H_2O/Zr(O\text{-}nC_3H_7)_4$ molar ratio=3~4, $C_2H_5OH/Zr(O\text{-}nC_3H_7)_4$=26.4~48.7 and $HNO_3/Zr(O\text{-}nC_3H_7)_4$=1.3~1.5 were easily drawn by hand. Initial pH of the solution is equal or lower than 0.8.

The gel fibers have diameter of 20~50 μm and length of greater than 50 cm. Also, no significant difference in fiberazibility was observed depending on the origin of stabilizers and their amounts.

2) From the analysis of XRD and Raman spectra

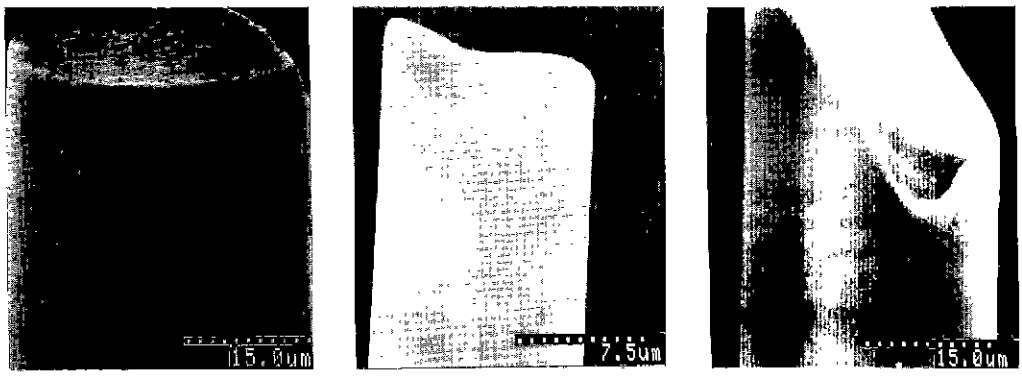

(a) (b) (c)

Fig. 12. Scanning electron micrographs of (a) Pure ZrO_2, (b) 2.5Y_2O_3-97.5ZrO_2 (mol%) fibers, and (c) 6CaO-94ZrO_2 (mol%) fibers (sintered at 1000℃ for 1 hr).

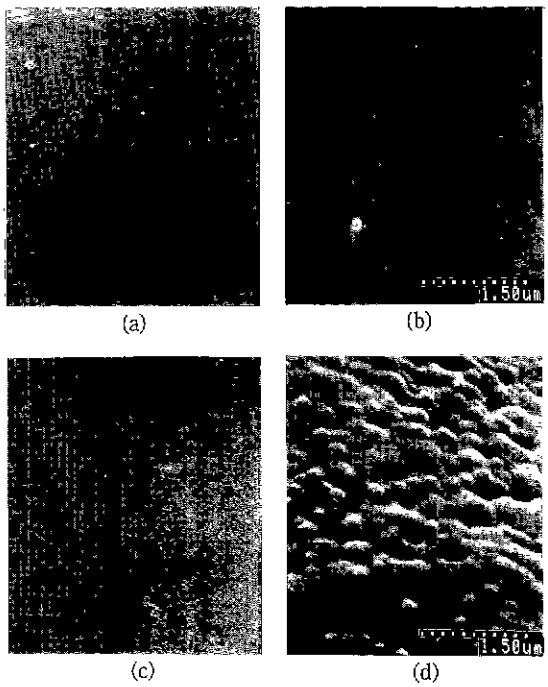

(a) (b)

(c) (d)

Fig. 13. Scanning electron micrographs of surface of (a) 2.5Y_2O_3-97.5ZrO_2 (1000℃), (b) 2.5Y_2O_3-97.5 ZrO_2 (1200℃), (c) 9CaO-91ZrO_2 (1000℃), and (d) 9CaO-91ZrO_2 (1200℃).

of pure ZrO_2 gel fibers heated at 800℃, we confirm the transformation of the tetragonal ZrO_2 to monoclinic ZrO_2

3) For Y_2O_3- and CaO-partially stabilized ZrO_2 fibers containing 3 mol% and 9 mol%, respectively, only tetragonal phase lasted up to 1000℃, and traces of monoclinic phase appeared at 1200℃.

4) The maximum tensile strength of Y_2O_3- and CaO-partially stabilized ZrO_2 fibers sintered at 1000℃ for 1 hr was about 1.3 and 2 GPa at diameter of 10~20 μm.

Acknowledgement

Financial support for this work from Inha university is gratefully acknowledged. We would also like to thank Dr. Kozuka and Mr. Hashimoto at the Institute for Chemical Research of Kyoto University for their helpful discussions in designing tensile strength measurement device.

REFERENCES

1. E. Leory *et al.*, "Fabrication of Zirconia Fibers from Sol-Gels," pp. 219-292 in Ultrastructural Processing of Ceramics, Glasses and Composites, Ed. by L.L. Hench and D.R. Ulrich, John-Wiley and Sons, New York, 1984.
2. K. Kamiya *et al*, "Preparation of Glass Fibres of the ZrO_2-SiO_2 and Na_2O-ZrO_2-SiO_2 Systems from Metal Alkoxide and their Resistance to Alkaline Solution," *J Mater Sci.*, **15**, 1765-1771 (1980).
3. T. Kokubo *et al.*, "Preparation of Amorphous ZrO_2 Fibers by Unidirectional Freezing of Gel," *J Non-Cryst. Solids*, **56**, 411-416 (1983).
4. S.M. Sim and D.E. Clark, "Preparation of Zirconia Fibers by Sol-Gel Method," *Ceram. Eng. Sci. Proc*, **10**(9-10), 1271-1282 (1989).

5. G. De *et al.*, "Zirconia Fibers from the Zirconium n-Propoxide-Acetylacetone-Water-Isopropanol System," *J. Mater. Sci. Lett.*, **9**, 845-846 (1990).
6. H. Kim *et al.*, "Preparation of ZrO_2 Fibers by Sol-Gel Process and its Properties," *J. Kor Ceram. Soc*, **23**(4), 78-84 (1986).
7. K. Kamiya *et al.*, "Preparation of Fibrous ZrO_2 and $CaO-ZrO_2$ from Zirconium Alkoxide by Sol-Gel Method," *Yogyo Kyokaishi* **92**(12), 1157-1163 (1987).
8. T. Yogo, "Synthesis of Polycrystalline Zirconia Fibre with Organozirconium Precursor," *J. Mater. Sci.*, **25**, 2394-2398 (1990).
9. C. Sakurai *et al.*, "Hydrolysis Method for Preparing Zirconia Fibers," *Ceram. Bull.*, **70**(4), 673-674 (1991).
10. C.M. Phillippi and K.S. Mazdiyasni, "Infrared and Raman Spectra of Zirconia Polymorphs," *J Am. Cream. Soc.*, **54**(5), 254-258 (1971).
11. V.G. Keramidas and W.B White, "Raman Scattering Study of the Crystallization and Phase Transformations of ZrO_2," *ibid.* **57**(1), 22-24 (1974).
12. M. Ishigame and T. Sakurai, "Temperature Dependence of the Raman Spectra of ZrO_2," *ibid.* **60**(7-8), 367-369 (1977).
13. C.H. Perry and D.W. Liu. "Phase Characterization of Partially Stabilized Zirconia by Raman Spectroscopy," *ibid*, **68**(8), C-184-C-187 (1985).
14. A. Feinberg and C.H. Perry, "Structure Disorder and Phase Transitions in ZrO_2-Y_2O_3 System." *J. Phys. Chem. Solids*, **42**, 513-518 (1981).
15. R.C. Garvie and P.S. Nicholson, "Phase Analysis Zirconia Systems," *J. Am Ceram. Soc.*, **55**(6), 303-305 (1972).
16. R.C. Garvie, "The Occurrence of Metastable Tetragonal Zirconia as a Crystallite Size Effect," *J. Phys Chem*, **69**(4), 1238-1243 (1965).
17. 橋本忠本, "ゾル-ゲル法によるガラス纖維作製の基礎と複合體へ の應用研究,"三重大學大學院 工學研究科 工業化學專攻 修士論文(平成 2年).
18. D.C. Bradley *et al.*, "Metal Alkoxide," Academic Press, London (1978).